# X-ray Absorption Spectra of $Cu^{II}$ and $Cu^{III}$ Complexes of *N*,*N*′-1,2-Phenylenebis(2-mercapto-2-methylpropionamide)

**Giampaolo Barone,[a] Gianfranco La Manna,[b] and Dario Duca*[a]**

**Keywords:** Copper / N,S ligands / X-ray absorption spectroscopy / Density functional calculations / Ab initio molecular orbital calculations

The X-ray absorption spectra of $Cu^{II}$ and $Cu^{III}$ complexes of *N*,*N*′-1,2-phenylenebis(2-mercapto-2-methylpropionamide) were recorded and analysed in solid phase. The EXAFS spectra of the two samples were refined with full multiple scattering path. Geometry optimisations on the $Cu^{II}$ and $Cu^{III}$ complexes were performed by the B3LYP density functional method, with the 6-31G(d,p) basis set, considering different spin multiplicities. The singlet state of the $Cu^{III}$ complex was shown to be more stable than the triplet state, and a good agreement between the calculated and the corresponding experimental structure was found. Further single-point calculations on the optimised geometry were carried out at the Hartree–Fock level for obtaining molecular orbital eigenvectors and eigenvalues. The latter were employed as parameters in a new fitting approach to rationalise the shape of the K-edge of the XAS spectra.


## Introduction

Stable mononuclear $Cu^{III}$ complexes of chelating ligands can be obtained by electrochemical oxidation of the corresponding $Cu^{II}$ complexes in solution.[1] The *N*,*N*′-1,2-phenylenebis(2-mercapto-2-methylpropionamide) $Cu^{II}$ and $Cu^{III}$ ions (Figure 1),[2] containing aliphatic thiolate groups in a square-planar coordination environment, can be considered as models of electron transfer copper proteins.[3−5]

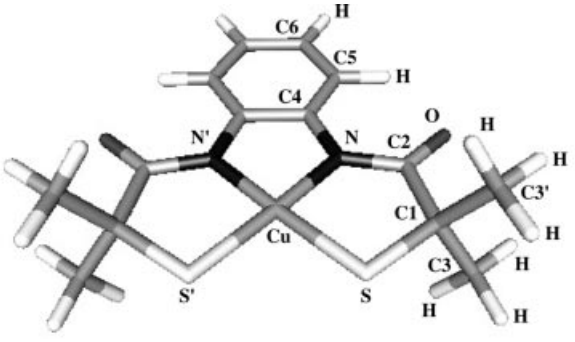


Figure 1. Structure of the square-planar $Cu^{II}$ and $Cu^{III}$ ionic systems considered in the B3LYP calculations

[a] Dipartimento di Chimica Inorganica e Analitica "S. Cannizzaro" dell'Università di Palermo
Viale delle Scienze, Parco d'Orleans II, 90128 Palermo, Italy
Fax: (internat.) + 39-091-427584
E-mail: dduca@unipa.it
[b] Dipartimento di Chimica Fisica "F. Accascina" dell'Università di Palermo
Viale delle Scienze, Parco d'Orleans II, 90128 Palermo, Italy

X-ray absorption spectroscopy (XAS) is used to determine electronic and geometric structures of the metal centres in metal-containing proteins and model systems.[6] Indeed, information on the local environment of the probe atom can be extracted with high accuracy, by utilising fine structure analysis. Moreover, the shape and position of the absorption edge help to distinguish different oxidation states of the metal atoms in analogous complexes.[7] In particular, in the rising edge of the XAS spectra of the copper complex, a few weak peaks and shoulders might originate from transitions from 1s to 3d or 4p orbitals, which are typically attributed to bound state forbidden transitions.[6] This information is usually employed to determine the local symmetry of the transition-metal environments.[8−12]

When discussing XAS spectra, two distinct pictures are introduced: i) the photoexcitation of core electrons to bound state energy levels, in the edge region: the X-ray absorption near edge spectrum (XANES), and ii) the backscattering of the photoejected core electrons, mainly in the high energy part of the spectrum, namely the extended X-ray absorption fine structure (EXAFS). Multiple scattering (MS) EXAFS analysis allows one to neglect the contributions of the excitation of the core electrons to the bound state energy levels. MS analysis has successfully been extended into the XANES region analysis.[13−15]

A recent study on $Cu^{II}$ and $Cu^{III}$ complexes[8] concluded that the shape of the corresponding K-edge region depends on the electronic properties and the coordination geometry of the chelating ligand. Moreover, a shift of about 2 eV was observed in the assigned resonances when going from $Cu^{II}$ to $Cu^{III}$ species.

  **DOI: 10.1002/ejic.200400495** 

The K-edge shape is usually very similar in complexes having the same ligands and different metal oxidation states.[7,8] The presence of three edge peaks was attributed to three electronic transitions involving the 1s, 3d and 4p orbitals of copper.[8] The positions and intensity of such transitions were evaluated by fitting the spectra and rationalised by empirical configuration interaction methods;[8] the parameters were obtained from X-ray photoelectron spectroscopy and XAS studies.

$Cu^{III}$ complexes, characterised by chelating sulfur groups, have been recently studied by XAS, confirming that the high-spin $d^8$ electron configuration of $Cu^{III}$ is stabilised by six bridged thiolate ligands.[16]

In the present work, the EXAFS spectra of the title complexes are shown, and an attempt to rationalise the XANES region by a new fitting procedure based on quantum mechanical information is carried out. For the latter, a qualitative picture of the transitions that are responsible for the XAS signals can be accomplished by the hopping of an electron from the lowest occupied molecular orbital to the lowest virtual ones,[17−19] within the frame of the orbital approximation, hence by employing a single-determinantal wave function. In the following fit procedure, the energetics determined in this way are used to reproduce the experimental XANES profile.

The necessary information from the electronic structure can be obtained by using quantum chemistry packages, such as G98W.[20] A more correct theoretical description should be given by overcoming the orbital approximation through the configuration interaction approach, for example by using recent versions of the CASSCF and CASPT2[21] methods. However, such algorithms are very time consuming, thus are not easily applicable to molecular systems of notable size, as those considered here.

## Results and Discussion

### 1. EXAFS Spectra

The $Cu^{III}$-phmi (see Exp. Sect.) EXAFS spectrum, together with its Fourier transform, is shown, as an example, in Figure 2. The interatomic distances were extracted from the extended X-ray absorption fine structure, by the full multiple scattering theory,[22] and shows good agreement with previous X-ray crystallographic studies.[2]

These distances are compared with crystallographic reference data in Table 1, which also shows the calculated structural parameters and the relative energy values of the $Cu^{II}$ and $Cu^{III}$ complexes, at the indicated spin multiplicity.

The B3LYP[23] energy of the closed shell $Cu^{III}$ compound was found to be 0.96 eV below the corresponding energy of the triplet spin state. The calculations for different spin states give rise to considerably different structural parameters (see Table 1). In the case of the $Cu^{III}$ compound, the calculated structural parameters of the singlet-state species mostly match the corresponding experimental ones. This allowed us to conclude that the $Cu^{III}$ compound is likely a singlet state, in agreement with the apparent absence of ESR signals.[2]

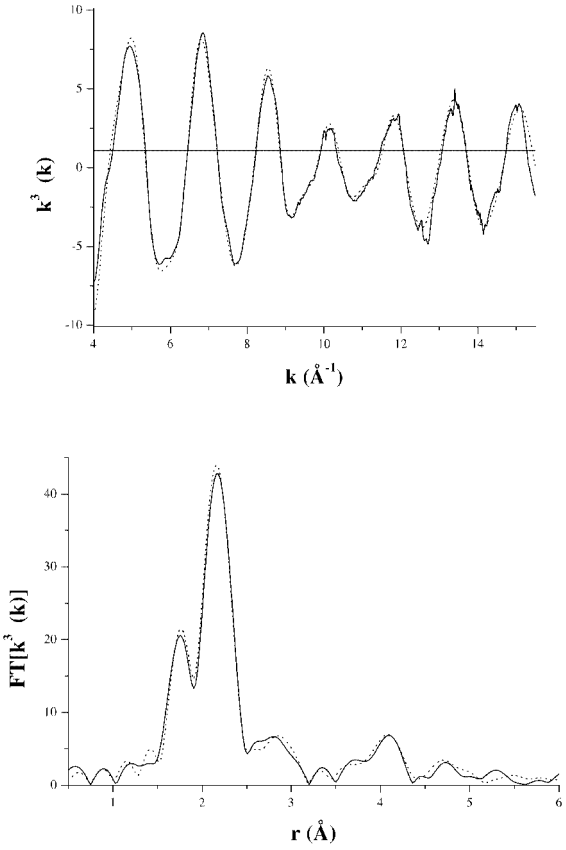


Figure 2. $k^2$-weighted EXAFS spectra and its fit (upper), $k^3\chi(k)$ vs. $k$, and the corresponding Fourier transforms (lower), FT[$k^3\chi(k)$] vs. $r$, of the $Cu^{III}$-phmi complex: the experimental and fit results are represented by the solid and dotted lines, respectively

Table 1. Distances and angles (Å and °), at given copper oxidation number (ON), obtained by geometry optimisation, at B3LYP/6-31G(d,p) level for different spin multiplicity (Spin), by X-ray crystallography[2] and by EXAFS analysis and calculated difference energy values $\Delta E$ (eV)

| | B3LYP/6-31G(d,p) | | | X-ray[2] | | EXAFS | |
|---|---|---|---|---|---|---|---|
| ON | III | III | II | III | II | III | II |
| Spin | 1 | 3 | 2 | – | – | – | – |
| Cu−N | 1.862 | 1.951 | 1.964 | 1.864 | 1.963 | 1.861 | 1.913 |
| Cu−S | 2.177 | 2.256 | 2.287 | 2.147 | 2.241 | 2.143 | 2.220 |
| Cu−C1 | 3.066 | 3.133 | 3.145 | 3.030 | 3.109 | 3.07 | 3.02 |
| Cu−C2 | 2.851 | 2.935 | 2.940 | 2.839 | 2.904 | 2.79 | 2.83 |
| Cu−C3 | 4.136 | 4.206 | 4.227 | 4.080 | 4.173 | 4.11 | 4.20 |
| Cu−O | 4.029 | 4.115 | 4.145 | 4.020 | 4.095 | 4.01 | 4.10 |
| Cu−C4 | 2.733 | 2.802 | 2.797 | 2.743 | 2.839 | 2.76 | 2.80 |
| Cu−C5 | 4.106 | 4.195 | 4.198 | 4.106 | 4.208 | 4.11 | 4.20 |
| Cu−C6 | 5.110 | 5.186 | 5.191 | 5.107 | 5.220 | 5.25 | 5.24 |
| N−Cu−N′ | 87.4 | 83.3 | 84.6 | 87.5 | 84.0 | – | – |
| S−Cu−S′ | 92.5 | 100.0 | 98.9 | 92.1 | 100.3 | – | – |
| S−Cu−N | 90.0 | 88.4 | 88.2 | 90.4 | 87.9 | – | – |
| S−Cu−N′ | 177.5 | 171.7 | 172.9 | 175.6 | 171.7 | – | – |
| $\Delta E$ | 0.00 | 0.96 | 4.77 | – | – | – | – |

Both theoretical and experimental data confirm that a change in the copper oxidation number from II to III de-

  

creases the metal−ligand distances of the atoms of the first coordination shell;[1,2,7,8] conversely, an increase in the spin multiplicity, at a given oxidation state of the metal, increases the same metal−ligand distances (see, for example, the calculated Cu−S or Cu−N distances).

## 2. K-edge Analysis

The K-edge region of both copper samples, together with their second derivative, is reported in Figure 3. In the inset, a portion of the low intensity pre-edge peak regions is highlighted. Two main changes are caused by the variation of the metal oxidation state: a) the position of the $Cu^{III}$ K-edge is, as previously reported for other complexes,[8] shifted by about 2 eV in the energy axis; b) the spectrum curve in the first peak region, at about 8979−8981 eV, is seemingly slightly lower in the $Cu^{II}$ sample; see the inset and the second derivative of the spectrum for details.

An attempt to interpret the K-edge transitions was carried out by using a molecular orbital (MO) Hartree−Fock (HF) description of the systems at the geometries previously optimised with the density functional (DFT) approach. This was needed to obtain reliable geometrical parameters through the DFT method and a further MO description, providing a set of HF eigenvalues to be used in our monoelectronic approach. In fact, the Kohn−Sham eigenvalues cannot be used for describing electronic vertical transitions.[24]

As reported in the Introduction, the edge electronic transitions were qualitatively described here in terms of hopping from the first occupied MO, which is essentially the 1s atomic orbital of the copper atom, to some of the lowest virtual MOs. Several approximations are inherent in this qualitative approach, orbital approximation and neglect of relativistic effects, inter alia.

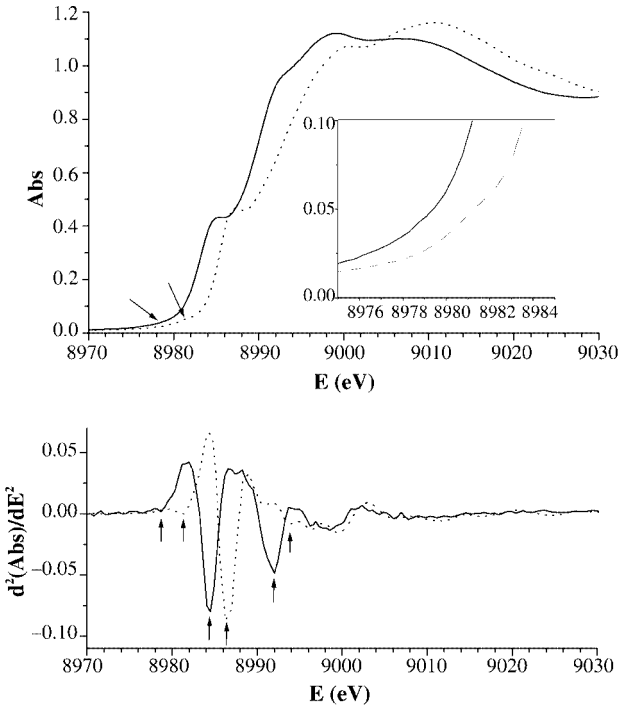


Figure 3. K-edge absorption Abs (upper) and its second derivative $d^2(Abs)/dE^2$ (lower) vs. the transition energy ($E$) of $Cu^{II}$-phmi (solid line) and $Cu^{III}$-phmi (dotted line); in the inset, a portion of the low intensity peak region is highlighted

Table 2. Eigenvalues differences E[MO($n$)] − E[MO(1)] (eV) and dipole strengths $D$ (a.u.) calculated for the electronic transitions involving the MO(1) and MO($n$) of the $Cu^{II}$ and $Cu^{III}$ systems

| | $Cu^{II}$ | | $Cu^{III}$ | |
|---|---|---|---|---|
| $n$ | E[MO($n$)] − E[MO(1)] | $D$ | E[MO($n$)] − E[MO(1)] | $D$ |
| 98 | 8954.25 | $2.0(2)\cdot10^{-12}$ | 8957.92 | $4.1(1)\cdot10^{-7}$ |
| 99 | 8954.44 | $3.3(7)\cdot10^{-7}$ | 8957.99 | $2.0(5)\cdot10^{-11}$ |
| 100 | 8954.68 | $3.8(1)\cdot10^{-4}$ | 8958.00 | $3.3(3)\cdot10^{-4}$ |
| 101 | 8954.72 | $3.7(4)\cdot10^{-9}$ | 8958.12 | $1.8(2)\cdot10^{-11}$ |
| 102 | 8955.58 | $2.7(4)\cdot10^{-8}$ | 8958.99 | $1.2(5)\cdot10^{-7}$ |
| 103 | 8955.71 | $4.7(9)\cdot10^{-12}$ | 8959.25 | $2.5(8)\cdot10^{-10}$ |
| 104 | 8956.73 | $1.5(5)\cdot10^{-5}$ | 8959.73 | $2.5(7)\cdot10^{-6}$ |
| 105 | 8956.90 | $4.4(6)\cdot10^{-12}$ | 8960.09 | $7.5(9)\cdot10^{-8}$ |
| 106 | 8956.94 | $7.4(8)\cdot10^{-8}$ | 8960.38 | $1.3(7)\cdot10^{-11}$ |
| 107 | 8957.05 | $1.5(8)\cdot10^{-6}$ | 8960.92 | $1.8(9)\cdot10^{-7}$ |
| 108 | 8957.55 | $1.2(6)\cdot10^{-4}$ | 8961.19 | $9.9(4)\cdot10^{-5}$ |
| 109 | 8957.69 | $4.8(8)\cdot10^{-9}$ | 8961.37 | $1.9(9)\cdot10^{-8}$ |
| 110 | 8958.09 | $7.2(2)\cdot10^{-8}$ | 8961.79 | $5.7(6)\cdot10^{-8}$ |
| 111 | 8958.25 | $6.4(6)\cdot10^{-5}$ | 8962.02 | $7.7(6)\cdot10^{-5}$ |
| 112 | 8958.35 | $4.6(0)\cdot10^{-8}$ | 8962.34 | $2.8(8)\cdot10^{-5}$ |
| 113 | 8958.68 | $4.5(3)\cdot10^{-5}$ | 8962.44. | $3.8(4)\cdot10^{-8}$ |
| 114 | 8958.71 | $4.8(5)\cdot10^{-14}$ | 8962.52 | $3.9(5)\cdot10^{-13}$ |
| 115 | 8958.78 | $1.0(2)\cdot10^{-8}$ | 8962.53 | $1.2(1)\cdot10^{-7}$ |
| 116 | 8959.02 | $2.3(5)\cdot10^{-8}$ | 8962.65 | $1.8(0)\cdot10^{-8}$ |
| 117 | 8959.29 | $6.0(8)\cdot10^{-8}$ | 8962.89 | $2.9(5)\cdot10^{-9}$ |
| 118 | 8959.54 | $3.2(6)\cdot10^{-12}$ | 8963.15 | $2.2(1)\cdot10^{-12}$ |
| 119 | 8959.67 | $6.9(6)\cdot10^{-7}$ | 8963.28 | $5.4(8)\cdot10^{-14}$ |
| 120 | 8959.91 | $3.8(1)\cdot10^{-17}$ | 8963.55 | $6.9(1)\cdot10^{-11}$ |

  

The dipole strengths, $D = |<MO(1)|\boldsymbol{r}|MO(n)>|^2$, connecting the first occupied MO and the virtual MOs of the $Cu^{II}$ and $Cu^{III}$ systems, were numerically calculated by a home-made code based on the VEGAS algorithm.[25]

The transition energy values were considered as the differences between the eigenvalues of MO(1) and MO(*n*), where $n = 98-120$. In the case of the $Cu^{II}$ complex, which is an open-shell system, only α-eigenvalues and eigenvectors were considered, but very similar values could be obtained by using the β-manifold. The values for the transition energies and *D* are reported in Table 2 for both $Cu^{II}$ and $Cu^{III}$ complexes.

Notably, in spite of the approximations introduced in the present treatment, the estimated frequency values for both compounds are just 0.3% lower than the experimental ones. Moreover, the transition energy values of the $Cu^{III}$ complex are shifted towards higher values by about 3 eV, with respect to the corresponding transitions of the $Cu^{II}$ complex, in line with the observed spectra. This is a clear indication that such a "naïve" treatment is able to account for the main features of the XAS spectrum.

Taking into account the results above, we tried to fit the experimental $Cu^{II}$-phmi and $Cu^{III}$-phmi XAS K-edge regions, considering the theoretical electronic transitions corresponding to the largest values of the *D* integrals. A single Gaussian function was assigned to each transition, having a full-width at half maximum (FWHM) equal to 1.5 eV and a height proportional to the corresponding *D* value. The resulting sets of $Cu^{II}$ and $Cu^{III}$ Gaussians were therefore two multifunction combs where the positions of the Gaussians were fixed by the DFT transition energies, and the relative intensities were modulated by the corresponding *D* values. Thus, the only two fit parameters, involving the core electronic transitions in both copper systems, were the position of the leading peak and its height.

One arctan function has been added in order to take into account the long-range trend of the EXAFS pattern, therefore, two more fit parameters are introduced. In fact, the arctan maximums, 1.1 (in absorption arbitrary units) both for the $Cu^{II}$ and $Cu^{III}$ systems, were qualitatively fixed by the analysis of the experimental spectra. The overall fitting process was finally performed within the 8950−9000 eV range, and the results are depicted in Figure 4. The good agreement between calculated and experimental spectra for both copper compounds is apparent ($R\chi^2 = 0.05$ and 0.15 for $Cu^{II}$ and $Cu^{III}$, respectively).

The area under the leading peaks of the $Cu^{II}$ and $Cu^{III}$ systems proved to be very similar, whereas the mean of the same leading peaks, in agreement with the experimental results, were shifted by about 2.5 eV. An analogous shift can be observed between the mean values of the arctan functions employed to fit the $Cu^{II}$ and $Cu^{III}$ complex spectra. These findings, supported by the observation that the arctan slope parameter is very similar in both systems [5.9(7) and 6.3(4) for $Cu^{II}$ and $Cu^{III}$ species, respectively] point out clearly that the proposed fit procedure is quite heuristic.

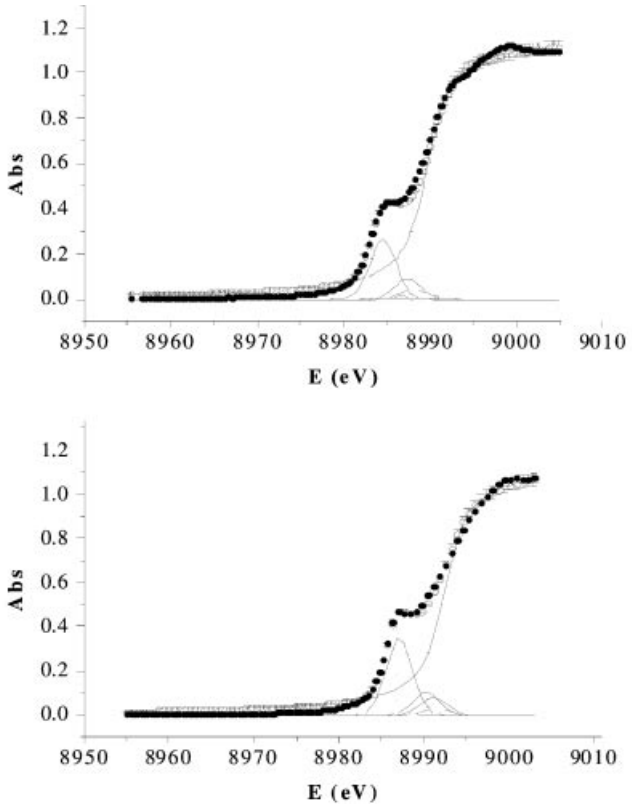


Figure 4. Fitting of the $Cu^{II}$-phmi (upper) and $Cu^{III}$-phmi (lower) XAS K-edge region: K-edge absorption Abs vs. transition energy *E*, experimental and fitting points are represented by filled and open circles, respectively; the continuous curves represent the fitting functions; the error bars (almost hidden and just visible on the points at higher energies), corresponding to the 2.5% of the fit values, visually show the agreement between experimental and fitted results

## Conclusion

EXAFS spectra enable information on the interatomic distances of the considered systems to be obtained. The whole set of the obtained geometrical results confirms the values already determined by using different experimental techniques, validating the possibility of performing EXAFS spectral analysis along with quantum mechanical calculations. Moreover, this approach is able to discriminate between the atomic oxidation numbers and the molecular spin states.

The K-edge region shape has been reproduced well by a simple quantum mechanical description of the core vertical transitions in the orbital approximation combined with an accustomed fitting procedure.

## Experimental Section

**General Remarks:** The XAS spectra on the K-edge of $(PPh_4)$-[Cu(*N*,*N*′-1,2-phenylenebis(2-mercapto-2-methylpropionamide)] ($Cu^{III}$-phmi) and $(NEt_4)_2$[Cu(*N*,*N*′-1,2-phenylenebis(2-mercapto-2-methylpropionamide)] ($Cu^{II}$-phmi) were recorded at the EMBL D2 bending magnet beam line of the DORIS storage ring (DESY,

  

Hamburg), running at 4.5 GeV and with a 50−100 mA ring current.

The samples were prepared by homogenising the powdered crystalline compounds (40 mg $Cu^{III}$-phmi and 30 mg $Cu^{II}$-phmi) in boron nitride and pressing the mixtures in 1-mm sample cells sealed with Kapton foil. The spectra were recorded at 20 K. Standard EXAFS analysis[26] was performed by the EXPROG[27] and EXCURVE98[22] programme packages. The full multiple scattering path was included in the fitting process of the molecular system. Its starting coordinates, excluding the hydrogen atoms, were taken from a previous X-ray crystallography study.[2]

**Electronic Structure Calculations and Fitting Procedure:** Quantum-mechanical calculations were performed at the B3LYP level, by the GAUSSIAN98 programme package,[20] by using the extended split-valence double-zeta 6-31G(d,p) basis set with full geometry optimisation.

The Cu oxidation states +2, with spin multiplicity of 2 for the complex, and +3, with spin multiplicities of 1 and 3, were considered. The calculations were performed by imposing $C_{2v}$ symmetry on the ionic complexes.

Further calculations at the HF level were carried out in order to obtain eigenvalues and eigenvectors of the MOs needed to evaluate vertical transition energies and dipole strengths.

The number of the considered virtual MOs, 23 for both $Cu^{II}$ and $Cu^{III}$ systems, corresponding to the number of the calculated transition moment integrals, was fixed to take into account the energy range of about 6 eV characterising the shoulder width in the K-edge rising region. The integral was calculated by a Fortran home-made code employing the Monte Carlo routine VEGAS along with the random number generator RAN2.[24] The reliability of the numerical integration procedure was verified by checking the *ortho*-normalisation condition of the MOs.

The fitting function, designed to mimic the XANES profile, was defined as in the following:

$$f = \arctan(h,\eta,\sigma) + g_p(h_p,\eta_p,\sigma_p) + \sum_i^n g_i(h_i,\eta_i,\sigma_i)$$

where $g_p$ and $g_i$ are Gaussian functions, simulating the pivot peak, i.e. the largest one, and $n$ minor peaks under the XANES profile. To reproduce the characteristic stepping behaviour of the latter, the arctan function was introduced.

The FWHM of all the Gaussians, $\sigma_p$ and $\sigma_i$, were fixed to 1.5 eV, whereas $h$, the arctan maximum value, was set to 1.1 (arbitrary absorption units). The values of $h_i$/(arbitrary absorption units) and $\eta_i$/eV were defined as $h_i = A_i h_p$ and $\eta_i = B_i + \eta_p$. The $A_i$ values corresponded to the calculated ratios between the dipole strength square of the given $i$th and the pivot transitions, whereas the $B_i$/eV parameters concerned the energy difference between the quantum mechanical and the fitting transition energy value, corresponding to the pivot peak.

Finally, $f$ was driven by four fitting parameters, $h_p$ (arbitrary absorption units), $\eta_p$ (eV), $\eta$ (eV) and $\sigma$ (eV), which are the other significant parameters fixed by the quantum mechanical calculations.

In the fitting procedure, the simplex AMOEBA[24] minimised the restricted chi-squared function:

$$R\chi^2 = \frac{1}{m < E >} \sum_k^m \frac{(C_k - E_k)^2}{E_k}$$

where $m$ is the number of experimental points considered in the fit, $E_k$ and $C_k$ the experimental and calculated absorptions and $<E>$ the average experimental absorption along the energy range analysed.

## Acknowledgments

This work was funded by the University of Palermo and by the Italian MIUR. The European Community supported G.B., contract HPRI-CT-1999−00017, within the frame of the Access to Research Infrastructure Action of the Improving Human Potential Programme to the EMBL Hamburg Outstation. Authors thank Prof. Björn Roos (University of Lund, Sweden) for fruitful discussions and Dr. Manuel Gnida (EMBL, Hamburg, Germany) for assistance in recording and analysing the EXAFS spectra.

[1] J. Hanss, A. Beckmann, H.-J. Krüger, *Eur. J. Inorg. Chem.* **1999**, 163−172.
[2] J. Hanss, H.-J. Krüger, *Angew. Chem. Int. Ed. Engl.* **1996**, *35*, 2827−2830.
[3] M. C. Machczynski, H. B. Gray, J. H. Richards, *J. Inorg. Biochem.* **2002**, *88*, 375−380.
[4] B. G. Malmström, P. Wittung-Stafshede, *Coord. Chem. Rev.* **1999**, *185−186*, 127−140.
[5] R. K Szilagyi, E. I Solomon, *Curr. Opin. Chem. Biol.* **2002**, *6*, 250−258.
[6] J. E. Penner-Hahn, *Coord. Chem. Rev.* **1999**, *190−192*, 1101−1123.
[7] T. Glaser, T. Beissel, E. Bill, T. Weyhermüller, V. Schünemann, W. Meyer-Klaucke, A. X. Trautwein, K. Wieghardt, *J. Am. Chem. Soc.* **1999**, *121*, 2193−2208.
[8] J. L. Du Bois, P. Mukherjee, T. D. P. Stack, B. Hedman, E. I. Solomon, K. O. Hodgson, *J. Am. Chem. Soc.* **2000**, *122*, 5775−5787.
[9] M. Gnida, R. Ferner, L. Gremer, O. Meyer, W. Meyer-Klaucke, *Biochemistry* **2003**, *42*, 222−230.
[10] L.-S. Kau, D. J. Spira-Solomon, J. E. Penner-Hahn, K. O. Hodgson, E. I. Solomon, *J. Am. Chem. Soc.* **1987**, *109*, 6433−6442.
[11] A. L. Roe, D. J. Schneider, R. J. Mayer, J. W. Pyrz, J. Widom, L. Que Jr., *J. Am. Chem. Soc.* **1984**, *106*, 1676−1681.
[12] T. E. Westre, P. Kennepohl, J. G. De Witt, B. Hedman, K. O. Hodgson, E. I. Solomon, *J. Am. Chem. Soc.* **1997**, *119*, 6297−6314.
[13] M. Benfatto, S. Della Longa, *J. Synchrotron Rad.* **2001**, *8*, 1087−1094.
[14] J. J. Rehr, R. C. Albers, *Rev. Mod. Phys.* **2000**, *72*, 621−654.
[15] A. Mijovilovich, W. Meyer-Klaucke, *J. Synchrotron Rad.* **2003**, *10*, 64−68.
[16] C. Krebs, T. Glaser, E. Bill, T. Weyhermüller, W. Meyer-Klaucke, K. Wieghardt, *Angew. Chem. Int. Ed.* **1999**, *38*, 359−361.
[17] F. A. Cotton, *Chemical Applications of Group Theory*, 3rd ed., Wiley-Interscience, New York, **1990**.
[18] M. Orchin, H. H. Jaffé, *Symmetry, Orbitals and Spectra (S. O. S)*, Wiley-Interscience, New York, **1971**.
[19] D. C. Haris, M. D. Bertolucci, *Symmetry and Spectroscopy*, Dover Publication, New York, **1989**.
[20] M. J. Frisch, G. W. Trucks, H. B. Schlegel, G. E. Scuseria, M. A. Robb, J. R. Cheeseman, V. G. Zakrzewski, J. A. Montgomery Jr., R. E. Stratmann, J. C. Burant, S. Dapprich, J. M. Millam, A. D. Daniels, K. N. Kudin, M. C. Strain, O. Farkas, J. Tomasi, V. Barone, M. Cossi, R. Cammi, B. Mennucci, C. Pomelli, C. Adamo, S. Clifford, J. Ochterski, G. A. Petersson, P. Y. Ayala, Q. Cui, K. Morokuma, D. K. Malick, A. D. Rabuck, K. Raghavachari, J. B. Foresman, J. Cioslowski, J. V. Ortiz, A.

  

G. Baboul, B. B. Stefanov, G. Liu, A. Liashenko, P. Piskorz, I. Komaromi, R. Gomperts, R. L. Martin, D. J. Fox, T. Keith, M. A. Al-Laham, C. Y. Peng, A. Nanayakkara, M. Challacombe, P. M. W. Gill, B. Johnson, W. Chen, M. W. Wong, J. L. Andres, C. Gonzalez, M. Head-Gordon, E. S. Replogle, J. A. Pople, *GAUSSIAN 98*, Revision A.8, Gaussian, Inc., Pittsburgh PA, **1998**.

[21] K. Pierloot, J. O. A. De Kerpel, U. Ryde, B. O. Roos, *J. Am. Chem. Soc.* **1997**, *119*, 218−226.

[22] N. Binsted, R. W. Strange, S. S. Hasnain, *Biochemistry* **1992**, *31*, 12117−12125.

[23] A. D. Becke, *J. Chem. Phys.* **1993**, *98*, 5648−5652.

[24] I. N. Levine, *Quantum Chemistry*, 5th ed., Prentice-Hall, Upper Saddle River, NJ, **2000**, p. 580.

[25] W. H. Press, S. A. Teukolsky, W. T. Vetterling, B. P. Flammery, *Numerical Recipes*, Cambridge University Press, Cambridge, **1992**.

[26] R. A. Scott, *Methods Enzymol.* **1985**, *111*, 414−459.

[27] H. F. Nolting, C. Hermes, EMBL Hamburg, **1992**.

Received June 9, 2004
Early View Article
Published Online November 24, 2004

  